Int. J. Multiphase Flow Vol. 13, No. 4, pp. 493–510, 1987
Printed in Great Britain.
0301-9322/87 $3.00 + 0.00

ANALYTICAL SOLUTIONS TO THE GRANULAR TEMPERATURE PROFILES AND EFFECTIVE PARTICLE-PHASE VISCOSITIES FOR SINGLE-BUBBLE MOTION IN A FLUIDIZED BED

A. R. NADKARNI and M. H. PETERS†
Department of Chemical Engineering and Environmental Engineering, Rensselaer Polytechnic Institute, Troy, NY 12180, U.S.A.

(*Received* 4 *September* 1985; *in revised form* 22 *December* 1986)

Abstract—We have considered asymptotic solutions at large bubble Reynolds number to the energy transport equation describing the spatial variation of the "granular temperature" in the flow field around a single bubble in a gas fluidized bed. The granular temperature represents the mean peculiar kinetic energy of the particle phase, and is necessary in a "complete" description of the fluid–particle transport phenomena. In the present case of single-bubble motion, the energy source is from the particle-phase viscous dissipation term. At large bubble Reynolds numbers, viscous effects are confined to a thin boundary-layer region, as in the case of a gas bubble in a liquid. It is demonstrated that the Prandtl number for this problem is $O(1)$, or that the momentum and "thermal" particle-phase boundary layers are of the same order of magnitude. The thermal boundary-layer equation for the granular temperature is subsequently derived and solved analytically. It is assumed that outside the thermal boundary layer, where viscous effects are negligible, the granular temperature is zero. From the mathematical solutions to the energy transport equation associated with single-bubble motion, including viscous dissipation terms and utilizing relationships from the kinetic theory of dense gases, we have given analytical expressions for the effective particle-phase shear viscosity and the effective particle-phase hydrostatic pressure, the two properties which characterize the kinetic component of the particle-phase pressure tensor. The theoretical results show remarkably good agreement with reported experimental measurements of the above properties.

1. INTRODUCTION

In a system of fluidized particles, the effective particle-phase viscosity and effective particle-phase pressure, the properties commonly used to represent the pressure tensor of the particle phase, are believed to play an important role in both the formation and steady motion of bubbles (e.g. Buyevich 1975; Weiland 1976; Homsy *et al.* 1980; Martin-Gautier & Pyle 1976; Liu 1983; Nadkarni 1985). A large effective viscosity of the particle phase in a gas fluidized bed is considered responsible for the shape of a fluidization bubble, by comparison with the shape–viscosity relationship for a gas bubble in a liquid (Davidson *et al.* 1977). One may also show, by asymptotic analyses of the governing transport equations, the dependence of other phenomena associated with bubble motion (such as patterns of gas and solid motion, bubble rise velocity and gas pressure distribution) on the bubble Reynolds number, defined on the basis of an effective particle-phase velocity (e.g. Weiland 1976; Nadkarni 1985).

In general, the total particle-phase pressure tensor in a fluid–particle system is thought to be composed of two parts, namely: one due to the force exerted by the surrounding fluid phase; and a second contribution due to direct interparticle interactions, i.e. collisions, electrical attractions and repulsions etc. [see the discussion in Rietema (1982)]. The former effect includes hydrodynamic interactions between particles and is, consequently, a configurationally-dependent quantity. The latter contribution has been "modeled" using dense-gas kinetic theory formulations [see, for example, Lun *et al.* (1984) and the references cited therein] and, thus, depends upon the local particle velocity–space distribution function. The applicability of kinetic theory descriptions to particles immersed in a host fluid may be at least partially quantified by analysis of the particle

†To whom all correspondence should be addressed, presently at: Department of Chemical Engineering, Florida State University, Tallahassee, FL 32316, U.S.A.

Stokes number, $N_{St} = \tau/t_0$, where τ is the particle relaxation time and t_0 is a characteristic time scale. The kinetic theory expressions, based upon particle motion in a vacuum, are applicable at large particle Stokes number (i.e. larger particle relaxation times). Assuming $\tau = \beta^{-1}$, where β is the Stokes friction coefficient divided by the particle mass, larger particle Stokes numbers can be shown to be more likely when the host fluid is a gas rather than a liquid. For example, in the case of fluidized particles, the characteristic time scale may be assumed to be given by the average interparticle spacing divided by the average particle speed, which is typically $O(10^{-2})$ s. Considering a 150 μm particle in a gas at standard conditions, we also have $\tau O(10^{-1})$ s, giving $N_{St}O(10^{1})$. In a liquid, on the other hand, $\tau O(10^{-3})$, shedding doubt on classical kinetic theory analogies for such systems. [A kinetic treatment applicable to liquid–particle systems may be found in a series of papers by Buyevich (1971, 1972a, b)]. In the case of collisions between fluidized particles, we may also rely upon the experimental results of Massimilla & Westwater (1960), as discussed by Meissner & Kusik (1970), to assume elastic collisions between particles. Consequently, we may write the kinetic contribution to the particle-phase stress tensor, $\mathbf{P}_p^k$, as (Hirschfelder *et al.* 1964, Chap. 9).

$$\mathbf{P}_p^k = -[p_p + (\tfrac{2}{3}\mu_p + \kappa_p)(\nabla\cdot\mathbf{v})]\,\mathbf{I} + 2\mu_p\,\mathrm{sym}\,(\nabla\mathbf{v}), \quad \text{for } \mathbf{P}_f > \mathbf{P}_f^{\min}, \qquad [1]$$

where $\mathbf{v}$ is the local mass averge velocity of the particles, p_p is the particle-phase pressure, μ_p and κ_p are the coefficients of the effective particle-phase shear viscosity and bulk viscosity, respectively, and $\mathbf{P}_f^{\min}$ is the minimum fluid-phase stress tensor required to set the particles in motion. It is clear that the rheology of the particle phase in a fluidized bed exhibits the presence of a "yield stress' necessary for the transition from a stagnant particle phase in a packed bed to a fluidized state. In the present study, we will always assume a fluid-like state of the particle phase. Equation [1] may be used in the solution to the transport equations for gas–particle systems at large Stokes numbers provided that the particle-phase properties μ_p, κ_p and p_p are specified. As discussed in detail by Lun *et al.* (1984), it therefore becomes necessary to introduce the so-called "granular temperature" and associated particle-phase energy transport equation. This equation describes the spatial and temporal variations in the mean peculiar kinetic energy of the particles upon which the particle-phase properties μ_p, κ_p and p_p depend.

It is the objective of the present study to obtain analytical expressions for the granular temperature, associated with single-bubble motion in an unbounded gas fluidized bed, from the solution to the particle-phase energy balance equation. The exact magnitudes of the particle-phase viscosity coefficient and particle-phase pressure associated with single-bubble motion have been the subject of much controversy and debate over the years (e.g. the majority of the studies on bubble motion neglect these terms entirely). Typical values of the bubble Reynolds number in a fluidized bed, defined on the basis of the bubble rise velocity and effective particle-phase properties, are large [$\sim$ 10 to 500; see Grace (1970)]. Therefore, we consider asymptotic solutions to the energy balance equation at large bubble Reynolds number. Under these conditions, viscous effects are confined to a thin region on the bubble surface, and both the momentum and thermal boundary-layer equations must be considered. Assuming that the particle-phase transport properties are constant in the boundary layer, it can be readily shown that Moore's (1963) solution for the fluid momentum boundary layer on a gas bubble in a liquid is applicable to the problem of bubble motion in fluidized particles (Appendix A). These resulting velocity fields are used in the thermal boundary-layer equations to obtain the granular temperature field near the bubble surface. Expressions for the granular temperature are presented for both the spherical and cylindrical bubbles, the latter being commonly studied in laboratory experiments. These expressions are then used to estimate values of the mean particle-phase shear viscosity and effective particle-phase pressure near the bubble surface. Finally, comparisons with relevant experimental data are made.

2. THE PARTICLE-PHASE ENERGY TRANSPORT EQUATION APPLIED TO SINGLE-BUBBLE MOTION IN AN UNBOUNDED FLUIDIZED BED

In the analysis of the single-bubble motion problem, we make the following assumptions:

(a) The particle volume fraction, ϕ, is assumed uniform in the dense phase external to the bubble. This assumption also implies that the particle phase is incompressible and the continuity equation

$$\nabla \cdot \mathbf{v} = 0 \qquad [2]$$

is applicable, where $\mathbf{v}$ is the local mean velocity of the particle phase.

(b) The effective particle-phase viscosity, μ_p, and conductivity, k_p, are assumed constant in the dense phase surrounding the bubble.

(c) We adopt a coordinate system which moves at the bubble velocity, and consequently consider the steady motion of the particles around the void or bubble.

(d) Additionally, any wall or end effects are neglected by considering single-bubble motion in an unbounded fluidized bed.

Under the above set of assumptions, and with the Newtonian form of the stress tensor in the particle phase, [1], the following general energy transport equation can be written [see, for example, Hirschfelder *et al.* (1964, Chap. 9)]:

$$\phi \rho_s c_p (\mathbf{v} \cdot \nabla T'_p) = k_p \nabla^2 T'_p + 2\mu_p (\mathbf{e}'_p \cdot \nabla \mathbf{v}), \qquad [3]$$

where T'_p is the so-called "granular temperature", defined by

$$\tfrac{3}{2} k_B T'_p = \tfrac{1}{2} m_p E\{|\mathbf{v}_p - \mathbf{v}|\}. \qquad [4]$$

In the above definition, we have assumed all the particles to be identical spheres, m_p being the mass of each particle, k_B is the Boltzmann constant, and $\mathbf{v}_p$ is the velocity of an individual particle. The term on the r.h.s. of [4] is the mean peculiar kinetic energy of the particles where the symbol "E" denotes an expected value. Also note in [3] that ρ_s is the solid material density, c_p is the "energy" capacity of the particle phase per unit mass, which for pure translational motion of the particles is given by

$$c_p = \frac{3}{2} \frac{k_B}{m_p}, \qquad [5]$$

and, finally, $\mathbf{e}'_p$ is the rate-of-strain tensor in the particle phase,

$$\mathbf{e}'_p = \nabla \mathbf{v} + \tilde{\nabla} \mathbf{v}. \qquad [6]$$

Applied to the problem of bubble motion, the boundary conditions necessary for the solution of [3] are given by

$$\frac{\partial T'_p}{\partial r'} = 0 \quad \text{at} \quad r' = r_b, \forall\, \theta, \qquad [7]$$

and

$$T'_p \to 0 \quad \text{as} \quad r \to \infty, \forall\, \theta, \qquad [8]$$

where r' represents the radial coordinate with reference to the bubble center of gravity, θ is the angular coordinate, which is taken as zero along the vertical axis of symmetry in the upper half of the bubble and increases in the clockwise direction, and r_b is the radius of the bubble which is either spherical or circular cylindrical. Equation [7] is derived from the fact that there is no normal particle mass or energy flux, across a "sharp" bubble surface. Equation [8] is representative of the fact that far from the bubble surface, where uniform or minimum fluidization conditions prevail, the particles are merely suspended in a fluid–particle dispersion and the mean peculiar velocity of the particles is assumed to be zero.

The energy transport equation [3] may be written in dimensionless form as

$$(\mathbf{V} \cdot \nabla T_p) = \frac{1}{\mathrm{Re\,Pr}} (\nabla^2 T_p) + \frac{2}{\mathrm{Re}} (\mathbf{e}_p : \nabla \mathbf{V}) \qquad [9]$$

with the boundary conditions

$$\frac{\partial T_p}{\partial r} = 0 \quad \text{at} \quad r = 1, \forall\, \theta, \qquad [10]$$

and

$$T_p \to 0 \quad \text{as} \quad r \to \infty, \forall\, \theta. \qquad [11]$$

The dimensionless variables and groups in [9] are defined as

$$r = \frac{r'}{r_b}, \qquad [12]$$

$$\mathbf{V} = \frac{\mathbf{v}}{u_b}, \qquad [13]$$

$$\boldsymbol{\Theta}_p = \frac{u_b}{r_b}\boldsymbol{\Theta}'_p, \qquad [14]$$

$$T_p = \frac{\frac{3}{2}k_B T'_p}{m_p u_b^2}, \qquad [15]$$

$$\mathrm{Re} = \frac{r_b u_b \phi \rho_s}{\mu_p} \qquad [16]$$

and

$$\mathrm{Pr} = \frac{c_p \mu_p}{k_p}, \qquad [17]$$

where u_b is the bubble rise velocity.

In the next section we consider asymptotic solutions to [9] at large bubble Reynolds numbers. In such flows viscous effects are confined to thin regions along the bubble surface, giving rise to both a momentum and thermal boundary layer. As shown in Appendix A, the momentum boundary-layer equations for the particle phase follow from Moore's (1963) solution for a gas bubble in a liquid. It will also be demonstrated that particle-phase viscous effects give rise to granular temperature gradients in the thermal boundary layer, serving as the only "source" for particle-phase energy production. Consequently, outside the thermal boundary layer, where viscous effects are negligible, the particle-phase energy or granular temperature may be assumed to be zero.

For completeness, we note that the problem of viscous dissipation in homogeneous fluids has been recently treated by Stewart & McCelland (1983) using local similarity variable transforms. Also, Acrivos & Goddard (1965) discussed the problem with respect to the Green's function method employed in their solutions to the thermal boundary-layer equation in a homogeneous fluid in the absence of viscous dissipation. Here we employ integral transform methods to obtain first-order solutions for the granular temperature behavior with viscous dissipation.

3. THE THERMAL BOUNDARY-LAYER EQUATION

3.1. *Spherical bubble*

Following the dense-gas kinetic theory (e.g. Hirschfelder *et al.* 1964), one may show that for pure translational motion of the particles and elastic particle–particle collisions, the Prandtl number, as defined in [17], is only a function of the particle volume fraction. The functional dependence is given by

$$\mathrm{Pr} = \frac{2}{5}\left\{\frac{1 + \frac{16}{5}\phi g(\phi) + 0.761[4\phi g(\phi)]^2}{1 + \frac{24}{5}\phi g(\phi) + 0.755[4\phi g(\phi)]^2}\right\},$$

where the function $g(\phi)$ is the contact equilibrium radial distribution function (see [65]). Typical values of the Prandtl number calculated from the above expression are

$$\mathrm{Pr}\,(\phi = 0.5) = 0.387$$

and

$$\mathrm{Pr}\,(\phi = 0.6) = 0.395.$$

Since the particle-phase Prandtl number, Pr, is $O(1)$, for the large bubble Reynolds number analysis we define a smallness parameter, ϵ, as

$$\epsilon = \frac{1}{\mathrm{Re\,Pr}}. \qquad [18]$$

Note that the product (Re Pr) is the particle-phase energy Péclet number, Pé. The dimensionless velocity functions for the particle flow around a spherical bubble are given by (Moore 1963) (Appendix A)

$$V_r = -\left(1 - \frac{1}{r^3}\right)\cos\theta + \epsilon_1 V_r^{(1)}(\xi, \theta) + \ldots \qquad [19]$$

and

$$V_\theta = \left(1 + \frac{1}{2r_3}\right)\sin\theta + \epsilon_1^{1/2} V_\theta^{(1)}(\xi, \theta) + \ldots, \qquad [20]$$

where $\xi = (r-1)\epsilon_1^{-1/2}$ and $\epsilon_1 = 1/\mathrm{Re}$. Note that since $\mathrm{Pr}O(1)$, we can consider $\epsilon_1 O(\epsilon)$ in the analysis given below. Substitution of the above equations into the axisymmetric spherical form of [9] gives the energy transport equation for the particle phase around a spherical bubble as

$$\left[-\cos\theta\left(1 - \frac{1}{r_3}\right) + \epsilon_1 V_r^{(1)}(\xi, \theta) + \ldots\right]\frac{\partial T_p}{\partial r} + \left[\frac{\sin\theta}{r}\left(1 + \frac{1}{2r^3}\right) + \frac{1}{r}\epsilon_1^{1/2} V_\theta^{(1)}(\xi, \theta) + \ldots\right]\frac{\partial T_p}{\partial \theta}$$
$$= \epsilon\left(\frac{\partial^2 T}{\partial r^2} + \frac{2}{r}\frac{\partial T_p}{\partial r} + \frac{1}{r^2}\frac{\partial^2 T_p}{\partial \theta^2} + \frac{\cot\theta}{r^2}\frac{\partial T_p}{\partial \theta}\right) + \frac{9\mathrm{Pr}\epsilon}{r^8}(3\cos^2\theta + \sin^2\theta) + \mathrm{HOT}, \qquad [21]$$

where HOT represents higher-order terms in the viscous dissipation function.

In the boundary layer ($r \to 1$), we introduce the stretched variable z, defined by (e.g. Kevorkian & Cole, 1980)

$$z = (r-1)\epsilon^{-m}, \quad m > 0. \qquad [22]$$

Using the above definition to replace r by z in [21], we obtain

$$-\cos\theta\,(3z - 6\epsilon^m z^2 + \ldots)\frac{\partial T_p^i}{\partial z} + \tfrac{3}{2}\sin\theta\,(1 - 2\epsilon^m z + \ldots)\frac{\partial T_p^i}{\partial \theta}$$
$$= \epsilon^{1-2m}\frac{\partial^2 T_p^i}{\partial z^2} + (2\epsilon^{1-m} - 2\epsilon z + 2\epsilon^{1+m} z^2 + \ldots)\frac{\partial T_p^i}{\partial z}$$
$$+ (\epsilon - 2\epsilon^{1+m} z + \ldots)\left(\frac{\partial^2 T_p^i}{\partial \theta^2} + \cot\theta\frac{\partial T_p^i}{\partial \theta}\right)$$
$$+ 9\mathrm{Pr}\,(\epsilon - 8\epsilon^{1+m} z + \ldots)(3\cos^2\theta + \sin^2\theta) + \mathrm{HOT}. \qquad [23]$$

The value of m is selected so that the convection and conduction terms are of the same order of magnitude as $\epsilon \to 0$; thus,

$$m = \tfrac{1}{2}. \qquad [24]$$

This result also shows that the momentum and thermal boundary layers are of the same order of thickness, consistent with $\mathrm{Pr} = O(1)$. Next we assume the following asymptotic expansion for T_p^i:

$$T_p^i = \sum_{n=0}^{\infty} \epsilon^n T^{(n)}(z, \theta) \qquad [25]$$

The differential equation for $T^{(0)}$ is obtained from [23] as $\epsilon \to 0$:

$$-3z\cos\theta\frac{\partial T^{(0)}}{\partial z}+\tfrac{3}{2}\sin\theta\frac{\partial T^{(0)}}{\partial\theta}=\frac{\partial^2 T^{(0)}}{\partial z^2},\quad \epsilon\to 0. \tag{26}$$

The boundary conditions applicable to [26] are

$$\frac{\partial T^{(0)}}{\partial z}=0 \quad \text{at} \quad z=0 \tag{27}$$

and

$$T^{(0)}\to 0 \quad \text{as} \quad z\to\infty \tag{28}$$

Equation [27] follows from [10]. The boundary condition [28] is based on the assumption of negligible viscous effects outside the thermal and momentum boundary layers.

One may show that the solution of [26] with the boundary conditions [27] and [28], is identically zero for all values of z and θ, i.e.

$$T^{(0)}(z,\theta)=0,\quad \epsilon\to 0. \tag{29}$$

The above result is also expected from physical considerations: the governing equation [26] does not contain the viscous dissipation source term. The following equation for $T^{(1)}$ is then obtained from [25] by taking the limit $\epsilon \to 0$:

$$-3z\cos\theta\frac{\partial T^{(1)}}{\partial z}+\tfrac{3}{2}\sin\theta\frac{\partial T^{(1)}}{\partial\theta}=\frac{\partial^2 T^{(1)}}{\partial z^2}+9\mathrm{Pr}(3\cos^2\theta+\sin^2\theta). \tag{30}$$

Note that only the zero-order velocity components contribute to the first-order energy equation. The boundary conditions for $T^{(1)}$ are identical to [27] and [28] for $T^{(0)}$.

Equation [30] can be conveniently solved by writing in terms of a new dependent variable, T^*, defined as

$$T^*(z,\theta)=T^{(1)}(z,\theta)-T^{(1)}(z,0). \tag{31}$$

For simplicity, let

$$S(z)=\frac{T^{(1)}(z,0)}{27\mathrm{Pr}}. \tag{32}$$

Equation [30] may then be written in terms of T^* and S as

$$\frac{\partial^2 T^*}{\partial z^2}+3z\cos\theta\frac{\partial T^*}{\partial z}-\tfrac{3}{2}\sin\theta\frac{\partial T^*}{\partial\theta}-81\mathrm{Pr}\,z\frac{\mathrm{d}S}{\mathrm{d}z}(1-\cos\theta)-18\mathrm{Pr}\sin^2\theta=0, \tag{33}$$

where the function $S(z)$ follows from [30] written along the axis $\theta=0$, i.e.

$$\frac{\mathrm{d}^2S}{\mathrm{d}z^2}+3z\frac{\mathrm{d}S}{\mathrm{d}z}+1=0 \tag{34}$$

with the following boundary conditions:

$$\frac{\mathrm{d}S}{\mathrm{d}z}=0 \quad \text{at} \quad z=0 \tag{35}$$

and

$$S\to 0 \quad \text{as} \quad z\to\infty. \tag{36}$$

The boundary conditions for T^* are

$$\frac{\partial T^*}{\partial z}=0 \quad \text{at} \quad z=0 \tag{37}$$

and

$$T^*\to 0 \quad \text{as} \quad z\to\infty. \tag{38}$$

The following additional condition results from the definition of the function T^* from [31]:

$$T^* = 0 \quad \text{at} \quad \theta = 0 \tag{39}$$

Equation [34] may be solved numerically for $S(z)$ with boundary conditions given by [35] and [36]. The results of a numerical solution are plotted in figure 1. The interfacial value of the function S is required for the calculation of the granular temperature at the bubble surface, which is (see figure 1)

$$S(0) = 1.91. \tag{40}$$

The solution of [33] with boundary conditions [37]–[39] is obtained by application of the Fourier cosine transformation (see Appendix B). Note that the function $\mathrm{d}S/\mathrm{d}z$ appearing in [33] is obtained by a single integration of [34] subject to condition [35]. The final result for the function $T^*(z, \theta)$ may be written as

$$T^*(z, \theta) = \mathrm{Pr}F(\xi, \theta), \tag{41}$$

where ξ is a subcharacteristic of [33], given by

$$\xi = z \sin^2 \theta. \tag{42}$$

The function $F(\xi, \theta)$ in [41] above is given by the following set of equations:

$$F(\xi, \theta) = \int_0^\theta [A_1(\xi, \theta, t) + A_2(\xi, \theta, t)]\, \mathrm{d}t, \tag{43}$$

where

$$A_1(\xi, \theta, t) = -\frac{6(2)^{\frac{1}{2}} \exp\left\{-\dfrac{\xi^2}{\frac{8}{3}[f(\theta) - f(t)]}\right\}}{\left\{\frac{8}{3}[f(\theta) - f(t)]\right\}^{\frac{1}{2}}} \tag{44}$$

and

$$A_2(\xi, \theta, t) = \frac{108}{\pi}\left(\frac{1 - \cos t}{\sin^5 t}\right)\int_0^\infty G(\alpha, t) \exp\{-\tfrac{2}{3}\alpha^2[f(\theta) - f(t)]\} \cos(\alpha\xi)\, \mathrm{d}\alpha, \tag{45}$$

and the functions $f(t)$ and $G(\alpha, t)$ are given by

$$f(t) = \tfrac{2}{3} - \tfrac{3}{4}\cos t + \tfrac{1}{12}\cos(3t) \tag{46}$$

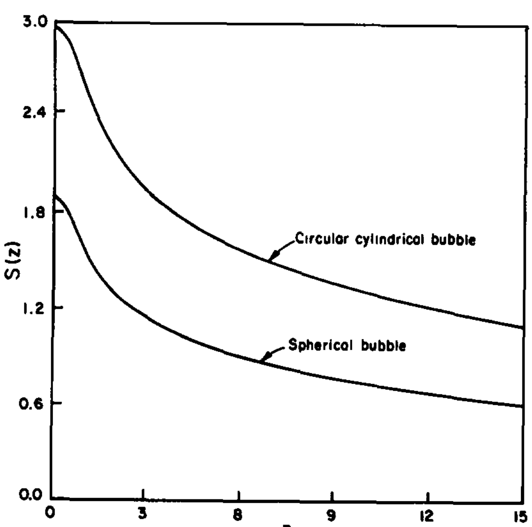

Figure 1. The function $S(z)$ for spherical and circular cylindrical bubbles.

and

$$G(\alpha, t) = \int_0^\infty \left\{ \int_0^x \exp\left[-\frac{3}{2} \frac{(x^2 - y^2)}{\sin^4 t} \right] dy \right\} x \cos(\alpha x)\, dx. \qquad [47]$$

We note that the integrals in [46] and [47] rapidly go to zero as the respective independent variables, α and x, increase. The above set of equations, [43]–[47], may therefore be solved using standard quadrature methods and by assigning sufficiently large numbers as upper limits of integration in [45] and [47].

An expression for the interfacial value of T^* is obtained quite simply from [33] as

$$T^*(0, \theta) = -12\mathrm{Pr}\,(1 - \cos\theta) \qquad [48]$$

and the expression for the granular temperature, T_p, may be written, correct to first order, as

$$\begin{aligned} T_p(z, \theta) &= \epsilon T(z, \theta) \\ &= (\mathrm{Re\ Pr})^{-1}\,[T^*(z, \theta) + T^{(1)}(z, 0)] \\ &= \mathrm{Re}^{-1}\,[F(z \sin^2\theta, \theta) + 27S(z)]. \end{aligned} \qquad [49]$$

Along the $\theta = 0$ axis, T_p is given by

$$T_p(z, 0) = 27\mathrm{Re}^{-1}S(z) \qquad [50]$$

The angular variation in T_p along the bubble surface is obtained from [48] and [49] as

$$T_p(0, \theta) = 27\mathrm{Re}^{-1}\,[S(0) - \tfrac{4}{9}(1 - \cos\theta)], \qquad [51]$$

which is shown in figure 2. Note that [49] has the feature of yielding a granular temperature of zero for an infinite bubble Reynolds number (i.e. non-viscous flow).

3.2. Circular cylindrical bubble

A solution for the case of a circular cylindrical bubble may be obtained in a similar manner. Substituting the large bubble Reynolds number velocity functions

$$V_r = -\left(1 - \frac{1}{r^2}\right)\cos\theta + \epsilon_1 V_r^{(1)}(\xi, \theta) + \dots \qquad [52]$$

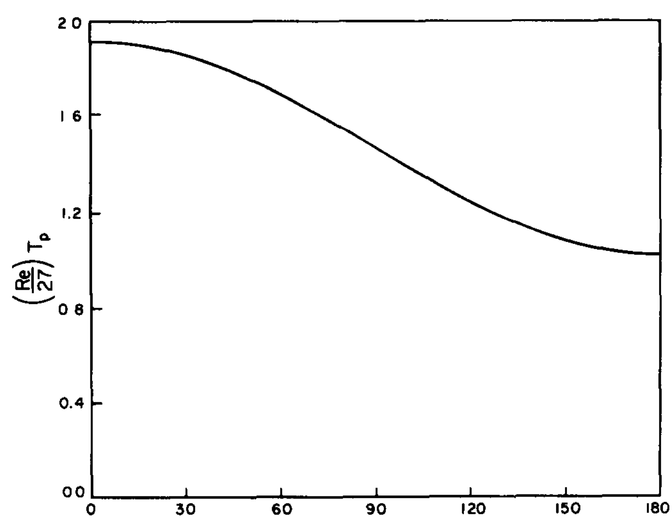

Figure 2. Variation of the granular temperature along the surface of a spherical bubble.

and

$$V_\theta = \left(1 + \frac{1}{r^2}\right)\sin\theta + \epsilon_1 V_r^{(1)}(\xi, \theta) + \dots \qquad [53]$$

into the cylindrical geometric form of the energy transport equation [9], the following equation is obtained (cf. [21]):

$$-\left[\left(1 - \frac{1}{r^2}\right)\cos\theta + \epsilon_1 V_r^{(1)}(\xi,\theta) + \dots\right]$$
$$+\left[\frac{1}{r}\left(1 + \frac{1}{r^2}\right)\sin\theta + \frac{1}{r}\epsilon_1^{1/2} V_\theta^{(1)}(\xi,\theta) + \dots\right]\frac{\partial T_p}{\partial\theta}$$
$$= \epsilon\left(\frac{\partial^2 T_p}{\partial r^2} + \frac{1}{r}\frac{\partial T_p}{\partial r} + \frac{1}{r^2}\frac{\partial^2 T_p}{\partial\theta^2}\right) + \frac{16\mathrm{Pr}\epsilon}{r^6} + \mathrm{HOT}. \qquad [54]$$

Following identical steps as for a spherical bubble, the relationship for the granular temperature, correct to first order, is obtained as

$$T_p(z,\theta) = (\mathrm{Re}\,\mathrm{Pr})^{-1}[T^*(z,\theta) + 16\mathrm{Pr}S(z)], \qquad [55]$$

where T^* follows from the solution to the equation

$$\frac{\partial T^*}{\partial z^2} + 2z\cos\theta\frac{\partial T^*}{\partial z} - 2\sin\theta\frac{\partial T^*}{\partial\theta} - 32\,(1-\cos\theta)\,z\frac{\mathrm{d}S}{\mathrm{d}z} = 0 \qquad [56]$$

with the boundary conditions given by [37]–[39]. For a circular cylindrical bubble, the function $S(z)$ appearing in [55] and [56] is obtained from the solution to the equation (cf. [34])

$$\frac{\mathrm{d}^2 S}{\mathrm{d}z^2} + 2z\frac{\mathrm{d}S}{\mathrm{d}z} + 1 = 0. \qquad [57]$$

The boundary conditions are again given by [35] and [36]. An expression for T^* is obtained by the application of Fourier cosine transformations to [56], leading to

$$T^*(z,\theta) = \mathrm{Pr}F(z\sin\theta,\theta), \qquad [58]$$

where

$$F(\xi,\theta) = -\frac{32}{\pi}\int_0^\theta \left(\frac{1-\cos t}{\sin^3 t}\right)\left\{\int_0^\infty G(\alpha,t)\exp\left[-\frac{\alpha^2}{2}(\cos\theta - \cos t)\right]\cos(\alpha\xi)\,\mathrm{d}\alpha\right\}\mathrm{d}t. \qquad [59]$$

The function $G(\alpha, t)$ in this case is given by

$$G(\alpha,t) = \int_0^\infty \left\{\int_0^x \exp\left[-\frac{(x^2-y^2)}{\sin^2 t}\right]\mathrm{d}y\right\}x\cos(\alpha x)\,\mathrm{d}x. \qquad [60]$$

Once again the integrals may be evaluated by standard quadrature methods. The function $S(z)$ which represents the variation of the granular temperature along the axis $\theta = 0$, is obtained from a numerical solution of [57] with the boundary conditions [35] and [36]. The result is shown in figure 1 with the interfacial value of the function $S(z)$ given as

$$S(0) = 2.96 \qquad [61]$$

and for the granular temperature field we obtain

$$T_p(z,\theta) = \mathrm{Re}^{-1}\,[F(z\sin\theta,\theta) + 16S(z)]. \qquad [62]$$

Equation [56] shows that, unlike the spherical bubble case, the granular temperature at the surface of a circular cylindrical bubble is uniform with respect to θ, i.e.

$$T_p(0,\theta) = 16\mathrm{Re}^{-1}S(0). \qquad [63]$$

4. ESTIMATION OF THE EFFECTIVE PARTICLE-PHASE VISCOSITY AND PRESSURE

In this section we apply the above results to estimate the effective particle-phase viscosity and pressure associated with single-bubble motion.

4.1. *Effective particle-phase shear viscosity*

For the hard-sphere model used here to represent particle–particle collisions, the kinetic theory expression for the shear viscosity, μ_p, is given by (Hirschfelder *et al.* 1964)

$$\mu_p = \frac{5}{16}\left[\frac{(\pi m_p k_B T_p')^{\frac{1}{2}}}{\pi d_p^2}\right]\frac{1}{g(\phi)}\{1 + \tfrac{16}{5}\phi g(\phi) + 0.761[4\phi g(\phi)]^2\}, \qquad [64]$$

where d_p is the particle diameter and $g(\phi)$ is the equilibrium radial distribution function evaluated at the point of contact of two colliding particles. For large values of the particle volume fraction ($\phi > 0.1$), and in the fluidized state of particles, this function may be estimated from the Carnahan–Starling equation of state for hard-sphere fluids (Carnahan & Starling, 1969):

$$g(\phi) = \frac{1 - \frac{\phi}{2}}{(1-\phi)^3}. \qquad [65]$$

We note from [64] that there is a spatial variation in the particle-phase shear viscosity corresponding to the spatial variation in granular temperature. On the other hand, the derivation of the granular temperature profile given in the last section was based upon the assumption of a uniform viscosity in the thermal boundary layer. Consequently, for estimation of a mean shear viscosity in the flow field surrounding a bubble, it is necessary to define a suitable average granular temperature. For this estimation purpose, we use the following simple definition of the average:

$$(T_p)_{av} = \frac{1}{\pi}\int_0^{\pi}\left[\frac{T_p(0,\theta) + T_p(\infty,\theta)}{2}\right]d\theta \qquad [66]$$

which gives, for a spherical bubble,

$$(T_p)_{av} = 19.8\left[\frac{(\mu_p)_{av}}{r_b u_b \phi \rho_s}\right] \quad \text{(spherical)} \qquad [67]$$

and for a circular cylindrical bubble,

$$(T_p)_{av} = 23.7\left[\frac{(\mu_p)_{av}}{r_b u_b \phi \rho_s}\right] \quad \text{(circular cylindrical)} \qquad [68]$$

Substitution of [67] and [68] into [64], gives the following relationship for the average particle-phase viscosity:

$$(\mu_p)_{av} = K\rho_s d_p^2\left(\frac{\bar{g}}{r_b}\right)^{\frac{1}{2}}\frac{[C(\phi)]^2}{\phi}, \qquad [69]$$

where the constant K depends upon the bubble geometry. For a spherical bubble,

$$K = 0.075 \quad \text{(spherical)} \qquad [70]$$

and for a circular cylindrical bubble,

$$K = 0.067 \quad \text{(circular cylindrical).} \qquad [71]$$

The constant $\bar{g}$ in [69] is the gravitational acceleration constant, and the function $C(\phi)$ is given by

$$C(\phi) = \frac{1}{g(\phi)}\{1 + \tfrac{16}{5}\phi g(\phi) + 0.761[4\phi g(\phi)]^2\}. \qquad [72]$$

Table 1. Calculated values of the average particle-phase shear viscosity, [69], and effective hydrostatic pressure, [77]

Particle diameter, d_p ($m \times 10^6$)	Bubble radius, r_b ($m \times 10^2$)	Particle volume fraction, ϕ	Solid density, ρ_s (kg/m^3)	Shear viscosity (P) Spherical bubble	Shear viscosity (P) Cylindrical bubble	Hydrostatic pressure (N/m^2) Spherical bubble	Hydrostatic pressure (N/m^2) Cylindrical bubble
200	5	0.55	2500	1.9	1.7	443	348
200	5	0.6	2500	4.4	3.9	1488	1169
400	10	0.6	2500	12.4	11.0	2955	2325
400	10	0.6	3000	14.8	13.2	3508	2790
400	20	0.6	3000	10.5	9.3	1766	1385

Note that in the derivation of [69], we have also made use of the following relationships for the bubble rise velocity:

$$u_b = \tfrac{2}{3}(r_b \bar{g})^{\frac{1}{2}} \quad \text{(spherical)} \qquad [73]$$

and

$$u_b = \tfrac{1}{2}(r_b \bar{g})^{\frac{1}{2}}. \quad \text{(circular cylindrical).} \qquad [74]$$

In table 1, we have listed values of the average particle-phase viscosity, estimated from [69], using representative values of the particle diameter, solid density, bubble radius and particle-phase volume fraction. It is to be noted that [69] shows the dependence of the effective particle-phase viscosity on the bubble geometry, i.e. the bubble size or bubble rise velocity, in addition to the system parameters such as particle diameter, particle volume fraction and solid density. This dependence on bubble characteristics is explained by the fact that the local "microscopic" particle motion and the resultant effective viscosity depend upon the source of perturbation; in this case the motion of the void.

In table 2, we have compared estimates of the particle-phase shear viscosity based on [69] with the estimates of Grace (1970) for the fluidization bubbles studied by Rowe & Partridge (1965). The results are presented for small fluidization bubbles only [which meet the criterion of negligible wall effects as given by Collins (1967)] in a bed of spherical ballotini particles with a narrow size range. Since [69] indicates a bubble-size-dependent viscosity, the results based on this equation are given as a range of viscosities for each particle size, corresponding to the range of bubble sizes observed in the experiments. The two sets of results show a good order of magnitude agreement. Table 2 also shows the estimates of particle-phase viscosities by Stewart (1968) and Schügerl *et al.* (1961), based on the experimental data of Rowe & Partridge (1965). Since these predictions are not obtained with respect to bubble motion in an unbounded bed, they cannot be compared with our results on a common basis. However, these estimates do predict viscosities in the same range as the analytical results.

4.2. *Particle-phase pressure*

The effective hydrostatic particle-phase pressure is related to the granular temperature by the

Table 2. Particle-phase viscosities associated with single-bubble motion

Particle size, d_p (μm)	Shear viscosities (P): Calculated from [69]	Estimated from bubble shapes (Grace 1970)	Based on the results of Schügerl *et al.* (1961) (from Stewart 1968)	Calculated by Stewart (1968)
550	43.9–52.0	9.5	—	26
460	25.9–30.7	—	12	18
220	10.0–11.8	8.5	9	8
170	5.1–6.0	7.5	8	8.5
140	3.4–4.1	8.0	8	2.5
120	2.1–2.5	8.5	8	7
82	0.85–1.0	9.0	6	1.5
60	0.37–0.44	7.0	4	7.5

Ballotini particles; bubble size, $r_b = 1.4$ cm maximum.

Table 3. Experimental measurements of particle-phase pressure (Meissner & Kusik 1970)

Bed material	Superficial gas velocity (m/s)	Particle-phase pressure (N/m^2)
Sand IV[a]	0.122	539
Sand IV[a]	0.143	786
Sand IV[a]	0.180	1325
Iron oxide[b]	0.293	477
Iron oxide[b]	0.323	755
Iron oxide[b]	0.390	1294
Iron oxide[b]	0.427	1602
Iron oxide[b]	0.463	1802

[a]Average particle diameter = 280 μm, minimum fluidization velocity = 0.082 m/s.
[b]Average particle diameter = 420 μm, minimum fluidization velocity = 0.283 m/s.

following relationship, resulting from the kinetic theory of dense gases (Hirschfelder *et al.* 1964):

$$p_p = \frac{6\phi k_B T_p'}{\pi d_p^3}[1 + 4\phi g(\phi)] \qquad [75]$$

or, in terms of the dimensionless granular temperature,

$$p_p = \tfrac{2}{3} T_p[1 + 4\phi g(\phi)](\phi \rho_s u_b^2). \qquad [76]$$

Knowing the spatial variation of T_p in the flow field surrounding a bubble, the spatial variation of p_p and its gradients can be calculated from the above equation for use in the particle-phase momentum balance equation (see Appendix A).

One may also calculate the averge particle-phase pressure in the flow field of a bubble based upon the average value of the granular temperature. Combining [75] and [64] an expression for the average particle-phase pressure is obtained:

$$p_p = \frac{1}{\pi \rho_s}\left[\frac{16(\mu_p)_{av}}{5d_p}\right]^2 \frac{\phi[1 + 4\phi g(\phi)]}{[C(\phi)]^2}, \qquad [77]$$

where $(\mu_p)_{av}$ may be calculated using [69]. We have given representative values of the particle-pressure, estimated from [77], in the last two columns of table 1.

Table 3 shows the experimental measurements of the particle-phase pressure obtained by Meissner & Kusik (1970). In these experiments, the particle-phase pressure was determined by measuring the reduction in weight of a hollow cylinder when partly submerged in a bubbling fluidized bed. Since Meissner & Kusik (1970) performed these measurements in vigorously bubbling beds (as evident from the high ratios of superficial gas velocity to minimum fluidization velocity), there is no common basis for comparison of these results to our estimates which are applicable to the flow field of a single isolated bubble. Nevertheless, there is a remarkable agreement between the magnitudes of particle-phase pressure measured experimentally and those calculated here using the concept of the granular temperature.

5. CONCLUSIONS

The interactions among particles in a perturbed fluid–particle system, such as the flow field around a bubble rising in a gas fluidized bed, result in gradients in the mean peculiar kinetic energies of the particles. The local mean peculiar kinetic energy of the particles is expressed in terms of the "granular temperature" which parallels the thermometric temperature, as defined in the kinetic molecular theory. The actual source of energy in the case considered here is from an effective particle-phase viscous dissipation term. Here we have considered approximate analytical solutions to the resulting energy transport equation, including viscous dissipation terms and as applied to the bubble motion problem, at large values of the particle-phase Péclet number (or, equivalently, large bubble Reynolds numbers).

Equations [49] and [62] give the asymptotic solutions for the dimensionless granular temperature at large bubble Reynolds number, correct to $O(\mathrm{Re}^{-1})$, for a spherical bubble and a circular cylindrical bubble, respectively. Since the bubble Reynolds number, defined on the basis of the bubble rise velocity and effective particle-phase properties, is typically large in magnitude (~ 10 to 500), the large Reynolds number analysis is of practical interest. Figures 1 and 2 show the radial variation of the granular temperature along the $\theta = 0$ axis and the angular variation at the bubble surface, respectively. Expressions from "classical" dense-gas kinetic theory may be used in conjunction with the calculated granular temperature to estimate average shear viscosity and effective hydrostatic pressure of the particle phase associated with bubble motion. Theoretical estimates based upon [69] and [77] are given in table 1 for some representative values of particle diameter, bubble size, particle volume fraction and solid density. These values may be compared with experimentally determined values of the effective viscosity and pressure, as shown in tables 2 and 3, respectively. The comparison shows that [69] and [77] predict the particle-phase properties to the correct order of magnitude.

The results obtained here may provide an important predictive tool for the behavior of fluidized particles, as the Enskog theory for "hard" spheres may be readily extended to include electrical interactions between particles [e.g. Coulombic repulsive and van der Waals' attractive forces (Ely & McQuarrie 1974; Stell *et al.* 1983)]. The *ad hoc* split of the total particle-phase pressure tensor into kinetic and configurational parts, the former of which is estimated from the assumption of particle motion in a vacuum, must await proper statistical mechanical formulations for complete justification of such approximations. For gas fluidized particles, the relatively large values of the particle relaxation time are most probably responsible for the success of the dense-gas kinetic theory formalism employed here.

Acknowledgement—M. H. P. would like to thank the National Science Foundation (NSF-CPE-8307384, Research Initiation Program) for support of this work.

REFERENCES

Acrivos, A. & Goddard, J. D. 1965 Asymptotic expansions for laminar forced-convection heat and mass transfer: Part I. Low speed flows. *J. Fluid Mech.* **23,** 273–291.

Buyevich, Y. A. 1971 Statistical hydromechanics of disperse systems. Part 1. Physical background and general equations. *J. Fluid Mech.* **49,** 489–507.

Buyevich, Y. A. 1972a Statistical hydromechanics of disperse systems. Part 2. Solution of kinetic equation for suspended particles. *J. Fluid Mech.* **52,** 345–355.

Buyevich, Y. A. 1972b Statistical hydromechanics of disperse systems. Part 3. Pseudo-turbulent structure of homogeneous suspensions. *J. Fluid Mech.* **56,** 313–336.

Buyevich, Y. A. 1975 A model of bubbles rising in a fluidized bed. *Int. J. Multiphase Flow* **2,** 337–351.

Carnahan, N. F. & Starling, K. E. 1969 Equations of state for nonattracting rigid spheres. *J. chem. Phys.* **51,** 635–636.

Collins, R. 1967 *J. Fluid Mech.* **28,** 97; cited in Grace (1970).

Davidson, J. F., Harrison, D. & Guedes de Carvalho, J. R. F. 1977 On the liquid-like behaviour of fluidized beds. *A. Rev. Fluid Mech.* **9,** 55–86.

Ely, J. F. & McQuarrie, D. A. 1974 Calculation of dense fluid properties via equilibrium statistical mechanical perturbation theory. *J. chem. Phys.* **60,** 4105–4108.

Grace, J. R. 1970 The viscosity of fluidized beds. *Can. J. chem. Engng* **48,** 30–33.

Hirschfelder, J. O., Curtiss, C. F. & Bird, R. B. 1964 *Molecular Theory of Gases and Liquids.* Wiley, New York.

Homsy, G. M., El-Kaissy, M. M. & Didwania, A. 1980 Instability waves and the origin of bubbles in fluidized beds—II. *Int. J. Multiphase Flow* **6,** 305–318.

Jackson, R. 1963 The mechanics of fluidized beds. Part 2. The motion of fully developed bubbles. *Trans Instn chem. Engrs* **41,** T22–T30.

Jackson, R. 1971 Fluid–Mechanical theory. In *Fluidization* (Edited by Davidson, J. & Harrison, D.). Academic Press, New York.

Kevorkian, J. & Cole, J. D. 1980 *Perturbation Methods in Applied Mathematics.* Springer, New York.

LIU, J. T. C. 1983 Nonlinear unstable wave disturbances in fluidized beds. *Proc. R. Soc. Lond.* **A389**, 331–347.
LUN, C. K. K., SAVAGE, S. B., JEFFERY, D. J. & CHEPURNIY, N. 1984 Kinetic theories for granular flow: inelastic particles in Couette flow and slightly inelastic particles in a general flowfield. *J. Fluid Mech.* **140**, 223–256.
MARTIN-GAUTIER, A. L. F. & PYLE, D. L. 1976 The fluid mechanics of single bubbles. In *Fluidization Technology*, Vol. 1 (Edited by KEAIRNS, D.). Hemisphere, Washington, D.C.
MASSIMILLA, L. & WESTWATER, J. W. 1960 Photographic study of solid–gas fluidization. *AIChE Jl* **6**, 134–138.
MEISSNER, H. P. & KUSIK, C. L. 1970 Particle velocities in a gas fluidized bed. *Can. J. chem. Engng* **48**, 349–355.
MOORE, D. W. 1963 The boundary layer on a spherical gas bubble. *J. Fluid Mech.* **16**, 161–176.
NADKARNI, A. R. 1985 Ph.D. Dissertation, Rensselaer Polytechnic., Inst., Troy, N.Y.
RIETEMA, K. 1982 Science and technology of dispersed two-phase systems—I & II. **37**, 1125–1150.
ROWE, P. N. & PARTRIDGE, B. A. 1965 An X-ray study of bubbles in fluidized beds. *Trans. Instn chem. Engrs* **43**, T157–T175.
SCHÜGERL, K. MERZ, M. & FETTING, F. 1961 *Chem. Engng Sci.* **15**, 1–99; cited in Grace (1970).
STELL, G., KARKHECK, J. & VAN BEIJEREN, H. 1983 Kinetic mean field theories: results of energy constraint in maximizing entropy. *J. chem. Phys.* **79**, 3166–3167.
STEWART, P. S. B. 1968 *Trans. Instn chem. Engrs* **46**, T60–T66; cited in Grace (1970).
STEWART, W. E. & MCCELLAND, M. A. 1983 Forced convection in three-dimensional flows: III. Asymptotic solutions with viscous heating. *AIChE Jl* **29**, 947–956.
WEILAND, R. M. 1976 A low-Reynolds-number analysis of gas bubbles in fluidized beds. *Ind. Engng Chem. Fundam.* **15**, 189–196.

APPENDIX A

The Particle-phase Momentum Conservation Equation and the Applicability of Moore's (1963) Solution

Under steady conditions and assuming a constant solids volume fraction, ϕ_0, in the dense phase surrounding the gas bubble, the mass and momentum transport equations can be written as follows:

Gas phase

Mass conservation

$$\nabla \cdot \mathbf{u} = 0. \quad [A.1]$$

Momentum conservation

$$-(1-\phi_0)\nabla p - \beta(\phi_0)(\mathbf{u}-\mathbf{v}) = 0. \quad [A.2]$$

Particle phase

Mass conservation

$$\nabla \cdot \mathbf{v} = 0. \quad [A.3]$$

Momentum conservation

$$\phi_0 \rho_s (\mathbf{v}\cdot\nabla)\mathbf{v} = -\nabla p_p + \mu_p \nabla^2 \mathbf{v} + \phi_0 \rho_s g - \nabla p. \quad [A.4]$$

In the above equations $\mathbf{u}$ is the local intrinsic-average gas velocity, p is the local intrinsic-average gas-phase pressure, p_p is the local volume-average particle-phase pressure and $\beta(\phi_0)$ is a volume-average drag coefficient. Equations [A.1]–[A.4] are identical to those given by Jackson (1963) with the addition of the Newtonian particle-phase stress tensor in [A.4].

We now wish to demonstrate the applicability of Moore's (1963) boundary-layer solution for liquid flow around a spherical gas bubble to the particle-phase flow associated with gas-bubble motion in a fluidized bed at large bubble Reynolds numbers.

The boundary conditions for the particle-phase motion can be written as

$$\mathbf{v} = -\mathbf{i}u_b \quad \text{as} \quad r' \to \infty, \qquad [A.5]$$

$$v_r = 0 \quad \text{at} \quad r' = r_b \qquad [A.6]$$

and

$$\mathbf{t}\cdot[\mathbf{e}_p'\cdot\mathbf{n}] = 0 \quad \text{at} \quad r' = r_b, \qquad [A.7]$$

where $\mathbf{i}$ is a unit vector in the direction of r' along $\theta = 0$, u_b is the bubble rise velocity, $\mathbf{t}$ and $\mathbf{n}$ represent unit tangent and unit normal vectors at a given point along the bubble surface and $\mathbf{e}_p'$ is the particle-phase rate-of-strain tensor [6]. Equation [A.5] is a consequence of the convected coordinate system necessary for steady-state conditions. Equation [A.7] is the zero tangential stress condition which cannot be satisfied by the corresponding potential flow solutions. Writing the particle-phase momentum equations in axisymmetric spherical coordinates, the r and θ components can be combined to eliminate the pressure and gravitational terms. Written in terms of the particle-phase stream function ψ, and in dimensionless form, the resulting equation is

$$\frac{1}{r^2}\frac{\partial(\psi, D_r^2\psi)}{\partial(r,\mu)} + \frac{2}{r^2}D_r^2\psi L_r\psi = -\mathrm{Re}^{-1}D_r^4\psi, \qquad [A.8]$$

where $\mu = \cos\theta$, $\mathrm{Re} = \dfrac{r_b u_b \phi \rho_s}{\mu_p}$,

$$D_r^2 = \left(\frac{\partial^2}{\partial r^2} + \frac{1-\mu^2}{r^2}\frac{\partial^2}{\partial \mu^2}\right) \qquad [A.9]$$

and

$$L_r = \left(\frac{\mu}{1-\mu^2}\frac{\partial}{\partial r} + \frac{1}{r}\frac{\partial}{\partial \mu}\right). \qquad [A.10]$$

In terms of the stream function ψ, the boundary conditions become

$$\psi = \tfrac{1}{2}r^2(1-\mu^2) \quad \text{as} \quad r \to \infty, \qquad [A.11]$$

$$\psi = 0 \quad \text{at} \quad r = 1, \qquad [A.12]$$

$$-\frac{(1-\mu^2)}{r^2}\frac{\partial^2\psi}{\partial\mu^2} + \left(\frac{\partial^2\psi}{\partial r^2} - \frac{2}{r}\frac{\partial\psi}{\partial r}\right) = 0 \quad \text{at} \quad r = 1 \qquad [A.13]$$

and

$$\frac{\partial\psi}{\partial r} = 0 \quad \text{at} \quad \mu = 1. \qquad [A.14]$$

The last condition accounts for the zero tangential velocity along the vertical axis of symmetry.

Equations [A.8]–[A.14] are precisely those considered by Moore (1963) in his boundary-layer analysis of gas-bubble motion in a liquid at large bubble Reynolds number, Re. In terms of the stream function, and to first order in Re^{-1}, Moore's composite solution can be written as

$$\psi = \frac{1}{2}\left(r^2 - \frac{1}{r}\right)\sin^2\theta - \mathrm{Re}^{-1}\psi_i^{(1)}(z,\theta), \qquad [A.15]$$

where

$$\psi_i^{(1)}(z,\theta) = -12\chi\sin^2\theta\int_0^{z/2\chi^{\frac{1}{2}}} f(t)\,\mathrm{d}t, \qquad [A.16]$$

$$f(t) = \pi^{-\frac{1}{2}}\exp(-t^2) - t\,\mathrm{erfc}(t) \qquad [A.17]$$

and

$$\chi(\theta) = \tfrac{2}{3}\operatorname{cosec}^4\theta\,(\tfrac{2}{3} - \cos\theta + \tfrac{1}{3}\cos^3\theta). \qquad [A.18]$$

The corresponding radial and tangential velocity fields are obtained from the definition of the stream function as

$$V_r = -\left(1 - \frac{1}{r^3}\right)\cos\theta + \mathrm{Re}^{-1} V_r^{(1)}[(r-1)\,\mathrm{Re}^{\frac{1}{2}}, \theta], \qquad [A.19]$$

where

$$V_r^{(1)}(z,\theta) = 2z\chi^{-\frac{1}{2}}(6\chi\cos\theta - 1) f\left(\frac{z}{2\chi^{\frac{1}{2}}}\right) - 8(3\chi\cos\theta - 1)\int_0^{z/2\chi^{\frac{1}{2}}} f(t)\,\mathrm{d}t \qquad [A.20]$$

and

$$V_\theta = \left(1 + \frac{1}{2r^3}\right)\sin\theta + \mathrm{Re}^{-\frac{1}{2}} V_\theta^{(1)}[(r-1)\,\mathrm{Re}^{\frac{1}{2}}, \theta], \qquad [A.21]$$

where

$$V_\theta^{(1)}(z,\theta) = -6\sin\theta\,\chi^{\frac{1}{2}} f\left(\frac{z}{2\chi^{\frac{1}{2}}}\right). \qquad [A.22]$$

The solutions for a circular cylindrical bubble are given in Nadkarni (1985).

APPENDIX B

Solution of [33]

For convenience [33] is rewritten below:

$$\frac{\partial^2 T^*}{\partial z^2} + 3z\cos\theta\frac{\partial T^*}{\partial z} - \frac{3}{2}\sin\theta\frac{\partial T^*}{\partial \theta} - 81\mathrm{Pr}\,z\frac{\mathrm{d}S}{\mathrm{d}z}(1-\cos\theta) - 18\mathrm{Pr}\sin^2\theta = 0. \qquad [B.1]$$

The boundary conditions are given by [37]–[39]:

$$\frac{\partial T^*}{\partial z} = 0 \quad \text{at} \quad z = 0, \qquad [B.2]$$

$$T^* \to 0 \quad \text{as} \quad z \to \infty \qquad [B.3]$$

and

$$T^* = 0 \quad \text{at} \quad \theta = 0. \qquad [B.4]$$

Let

$$f_1(z) = z\frac{\mathrm{d}S}{\mathrm{d}z}, \qquad [B.5]$$

where the term

$$\frac{\mathrm{d}S}{\mathrm{d}z}$$

is obtained by a one-step integration of [34] with the boundary condition [35], giving

$$\frac{\mathrm{d}S}{\mathrm{d}z} = -\int_0^z \exp[-\tfrac{3}{2}(z^2 - z^{*2})]\,\mathrm{d}z^*. \qquad [B.6]$$

By defining

$$\xi = z\sin^2\theta \qquad [B.7]$$

and transforming [B.1] from (z,θ) space to (ξ,θ) space, we obtain

$$\sin^4\theta\frac{\partial^2 F}{\partial \xi^2} - \frac{3}{2}\sin\theta\frac{\partial F}{\partial \theta} - 81(1-\cos\theta) f_1\left(\frac{\xi}{\sin^2\theta}\right) - 18\sin^2\theta = 0, \qquad [B.8]$$

where

$$F(\xi, \theta) = \frac{T^*(z, \theta)}{\mathrm{Pr}}. \qquad [B.9]$$

Let

$$H(\alpha, \theta) = F_c[F(\xi, \theta)], \qquad [B.10]$$

where the operator F_c denotes the Fourier cosine transform operator and α is the transform variable. Carrying out the Fourier cosine transform of each term of [B.8] and using the identity

$$F_c\left(\frac{\partial^2 T^*}{\partial \xi^2}\right) = -\left(\frac{2}{\pi}\right)^{\frac{1}{2}}\left(\frac{\partial T^*}{\partial z}\right)_{z=0} - \alpha^2 H(\alpha, \theta) \qquad [B.11]$$

$$= -\alpha^2 H \text{ (applying boundary condition [B.2])}, \qquad [B.12]$$

we obtain the following equation:

$$\sin^4\theta(-\alpha^2 H) - \tfrac{3}{2}\sin\theta\frac{\partial H}{\partial\theta} - 81(1-\cos\theta)F_c\left[f_1\left(\frac{\xi}{\sin^2\theta}\right)\right] - 18\sin^2\theta = 0 \qquad [B.13]$$

which gives, upon rearrangement,

$$\frac{\partial H}{\partial\theta} + (\tfrac{2}{3}\alpha^2\sin^3\theta)H = -54\frac{(1-\cos\theta)}{\sin\theta}F_c\left[f_1\left(\frac{\xi}{\sin^2\theta}\right)\right] - 12\sin\theta. \qquad [B.14]$$

The solution of [B.14] may be written at once as

$$H(\alpha, \theta) = \exp[-\tfrac{2}{3}\alpha^2 f(\theta)]\left\{-54\int_0^\theta\left(\frac{1-\cos t}{\sin t}\right)F_c\left[f_1\left(\frac{\xi}{\sin^2 t}\right)\right]\exp[\tfrac{2}{3}\alpha^2 f(t)]\,dt\right.$$
$$\left. - 12\int_0^\theta \sin t\exp[\tfrac{2}{3}\alpha^2 f(t)]\,dt\right\}, \qquad [B.15]$$

where

$$f(t) = \int_0^t \sin^3 t^*\,dt^* \qquad [B.16]$$

$$= \tfrac{2}{3} - \tfrac{3}{4}\cos t + \tfrac{1}{12}\cos 3t \qquad [B.17]$$

and

$$F_c\left[f_1\left(\frac{\xi}{\sin^2 t}\right)\right] = -\left(\frac{2}{\pi}\right)^{\frac{1}{2}}\int_0^\infty\left\{\frac{\xi}{\sin^2 t}\right.$$
$$\times\left.\int_0^{\frac{\xi}{\sin^2 t}}\exp\left[-\frac{3}{2}\left(\frac{\xi^2}{\sin^4 t} - z^{*2}\right)\right]dz^*\right\}\cos(\alpha\xi)\,dz \qquad [B.18]$$

$$= -\frac{1}{\sin^4 t}\left(\frac{2}{\pi}\right)^{\frac{1}{2}}G(\alpha, t), \qquad [B.19]$$

where

$$G(\alpha, t) = \int_0^\infty\left\{\int_0^x \exp\left[\frac{-\frac{3}{2}(x^2-y^2)}{\sin^4 t}\right]dy\right\}x\cos(\alpha x)\,dx. \qquad [B.20]$$

Substituting [B.18] into [B.14], we obtain

$$H(\alpha, \theta) = 54\left(\frac{2}{\pi}\right)^{\frac{1}{2}}\int_0^\theta\left(\frac{1-\cos t}{\sin^5 t}\right)G(\alpha, t)\exp\{-\tfrac{2}{3}\alpha^2[f(\theta)-f(t)]\}\,dt$$
$$-12\int_0^\theta \sin t\exp\{-\tfrac{2}{3}\alpha^2[f(\theta)-f(t)]\}\,dr. \qquad [B.21]$$

The function $F(\xi, \theta)$ is obtained by taking the inverse cosine transform of the above equation, which gives

$$F(\xi, \theta) = \frac{108}{\pi} \int_0^{\infty} \left[\int_0^{\theta} \left(\frac{1 - \cos t}{\sin^5 t} \right) G(\alpha, t) \exp\{ -\tfrac{2}{3}\alpha^2[f(\theta) - f(t)]\} \, dt \right] \cos(\alpha\xi) \, d\alpha$$
$$- 12\left(\frac{2}{\pi}\right)^{1/2} \int_0^{\infty} \left[\int_0^{\theta} \sin t \exp\{ -\tfrac{2}{3}\alpha^2[f(\theta) - f(t)]\} \, dt \right] \cos(\alpha\xi) \, d\alpha. \qquad [B.22]$$

Changing the order of integration and simplifying the second term on the r.h.s. further, we obtain

$$F(\xi, \theta) = \int_0^{\theta} [A_2(\xi, \theta, t) + A_1(\xi, \theta, t)] \, dt, \qquad [B.23]$$

where the functions $A_1(\xi, \theta, t)$ and $A_2(\xi, \theta, t)$ are given by [44] and [45], respectively.